Vol 14 No 7, July 2005
1009-1963/2005/14(07)/1378-04

Chinese Physics

© 2005 Chin. Phys. Soc.
and IOP Publishing Ltd

Absolute oscillator strength densities below 100eV of N_2*

Sun Jian-Min(孙建敏)[a], Zhong Zhi-Ping(钟志萍)[b], Zhu Lin-Fan(朱林繁)[a]†, Liu Xiao-Jing(刘小井)[a], Yuan Zhen-Sheng(苑震生)[a], and Xu Ke-Zun(徐克尊)[a]

[a] *Hefei National Laboratory for Physical Sciences at Microscale, Department of Modern Physics, University of Science and Technology of China, Hefei 230026, China*

[b] *Department of Physics, Graduate School of the Chinese Academy of Sciences, Beijing 100039, China*

(Received 25 November 2004; revised manuscript received 10 January 2005)

The absolute optical oscillator strength density (OOSD) and generalized oscillator strength densities (GOSDs) below 100eV of N_2 are determined with an incident electron energy of 2500eV and an energy resolution of 100 meV. The absolute generalized oscillator strengths (GOSs) for two transitions to the superexcited states at 23 and 31.4eV are determined and their momentum transfer dependence behaviours are discussed.

Keywords: oscillator strength, superexcited state, energy-loss spectrum
PACC: 3270C, 3150, 3450B

1. Introduction

Nitrogen is a significant component in the Earth's upper atmosphere, it also has significant role in N_2 laser and a variety of gaseous discharge processes, so its oscillator strengths and differential cross sections (DCSs) for the valence shell excitation have extensive application in many areas, e.g. plasma physics, astrophysics, laser science etc.

Oscillator strengths and DCSs of N_2 have been extensively studied both experimentally and theoretically. Previous investigations of optical oscillator strength up to 1995 have been reviewed by Chan *et al*,[1] and Xu *et al.*[2] However, the reported absolute optical oscillator strength density (OOSD) with high energy resolution was limited to the 12–22eV energy loss region. Most previous investigations of DCSs were carried out at lower incident electron energies, and recently their results were summarized by Brunger and Buckman.[3] At higher incident electron energies of 25 and 33 keV, the absolute generalized oscillator strength densities (GOSDs) between 15–50eV and the absolute generalized oscillator strengths (GOSs) in the momentum transfer square K^2 region of 0.5–5.08 a.u. for the dipole-forbidden transition at 31.4eV were measured by Lee *et al.*[4] Recently, the GOS for the 31.4eV transition was determined at 1 keV electron impact energy, and under the first Born approximation it was also calculated with ab initio configuration-interaction target wavefunctions.[5] To the best of our knowledge, no high energy resolution GOSD for a broad region has been published up to now. In the present work, the absolute OOSD and GOSDs with high energy resolution up to 100eV have been determined, and the absolute GOSs for two transitions to the superexcited states at 23 and 31.4eV are reported, of which the GOSs for the transition to the superexcited state at 23eV are determined for the first time, and its momentum transfer dependence behaviour is discussed.

2. Experimental method

The angle-resolved electron-energy-loss spectrometer used in this work has been described in detail in Refs.[6–11]. Briefly, it consists of an electron gun, a hemispherical electrostatic monochromator made of aluminium, a rotatable energy analyser of the same type, an interaction chamber, a number of cylindrical electrostatic lenses, and a one-dimension position sensitive detector for detecting the scattered electrons.

*Project supported by the National Natural Science Foundation of China (Grant Nos 10474089, 10134010 and 10004010).
†E-mail: lfzhu@ustc.edu.cn

All of these components are enclosed in four separate vacuum chambers made of stainless steel. The impact energy of the spectrometer can be varied from 1 to 5keV. For the present experiment it was set at 2.5keV and the energy resolution was about 100meV. The background pressure in the vacuum chamber was 5×10^{-5}Pa. When the gas sample was introduced, the pressure in the reaction chamber rose to 8×10^{-3}Pa. The true zero angle was calibrated by the symmetry of the angular distribution of the inelastic scattering signals of $a''^1\Sigma_g^+ \leftarrow X\ ^1\Sigma_g^+$ around the geometry nominal 0°. The angular resolution was about 0.8° (fwhm) at present.

The electron energy loss spectra of N_2 were measured in the scattering angle range of 0°–6° with an interval of 2°. The energy of the spectra was calibrated to the $a''^1\Sigma_g^+(\nu'=0)$ (12.257eV).[2] Then, the spectrum measured at a mean angle of 0° was converted into the relative OOSD spectrum by multiplying by the Bethe–Born conversion factor of the spectrometer.[6,12] The spectra at other scattering angles were converted into the relative GOSD spectra, which is defined as (in atomic units)[13,14]

$$\frac{\mathrm{d}f(E,K)}{\mathrm{d}E}=\frac{E}{2}\frac{p_0}{p_a}K^2\frac{\mathrm{d}^2\sigma}{\mathrm{d}E\mathrm{d}\Omega}. \qquad (1)$$

Here $\mathrm{d}f(E,K)/\mathrm{d}E$ and $\mathrm{d}^2\sigma/(\mathrm{d}E\mathrm{d}\Omega)$ represent the GOSD and double differential cross section (DDCS), respectively. E and K are the excitation energy and momentum transfer while p_0 and p_a are the incident and scattered electron momenta, respectively.

The relative OOSD was normalized to the absolute one at 50eV reported by Chan *et al.*[1] The relative GOSD spectra were made absolute by the valence shell Bethe sum-rule:[14,15]

$$S_{\mathrm{val}}(0)=N_{\mathrm{val}}+N_{\mathrm{PE}}=\int_{E'}^{\infty}\left(\frac{\mathrm{d}f}{\mathrm{d}E}\right)\mathrm{d}E, \qquad (2)$$

where N_{val} is the total number of valence electrons in the target molecule (10 for N_2), N_{PE} is a small correction (0.3 for N_2) estimated by the Pauli-excluded transitions from the K shells to the already occupied valence shell orbitals,[16,17] and E' is the lowest excitation energy. In the sum-rule normalization procedure, the intensity of the relative GOSD at a definite scattering angle was first numerically integrated over a measured energy loss range, i.e. up to 78eV for 2° and 4°, 98eV for 6°. Then the remaining intensity was estimated by the integral of a fitted function AE^{-B} (E is energy, A and B are the best fitted parameters) from the limit of the measurements to infinity. Here the empirical constants A and B were determined by least–squares fitting to the experimental data in the energy loss range of 58–78eV for 2°, 61–78eV for 4°, and 75–98eV for 6°.

The present experimental errors mainly come from the uncertainties of the statistical counts, the angular and energy position's determination, the least-squares fitting procedure to obtain the intensity higher than the measured energy region, and the fitting procedure to obtain the areas of the peaks. The absolute GOSs for two transitions to the superexcited states at 23 and 31.4eV were determined by fitting the absolute GOSDs with the background subtracted. The total errors are shown in the corresponding figures.

3. Results and discussion

Figure 1 shows the present absolute OOSD spectrum and the previous experimental one[1] determined by the same method as ours but with higher impact energy of 8 keV and lower energy resolution of 1eV. It can be seen that the present measured spectrum above 18eV is in good agreement with the previous experimental one.[1] The difference in the energy region below 18eV (see the inset in Fig.1) can be due to the different energy resolution.

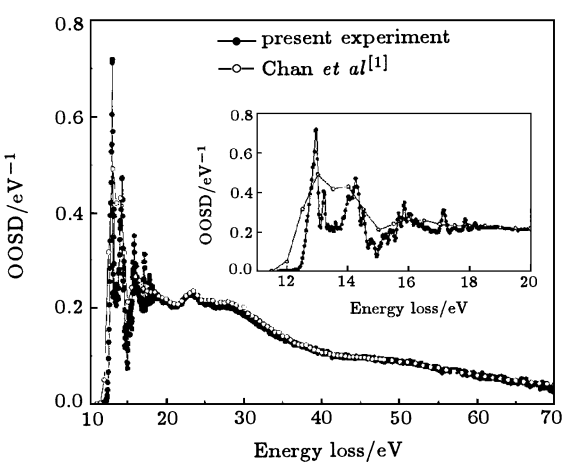


Fig.1. Absolute OOSD spectrum of N_2 in the energy region of 10–70eV. The inset shows the expanded spectra in the energy region of 11–20eV.

Figure 2 shows the present absolute GOSD spectra at the scattering angles of 0°, 2°, 4° and 6°. Note that with the increasing of K^2, the energy position of the very broad feature observed at the scattering angles of 4° and 6°, i.e. the Bethe ridge, moves to higher energy loss and the corresponding width becomes more diffuse. Such phenomena have also been observed by us in other molecules such as NO[18] and

O_2.[19] Furthermore, two broad peaks marked as α and β were observed.

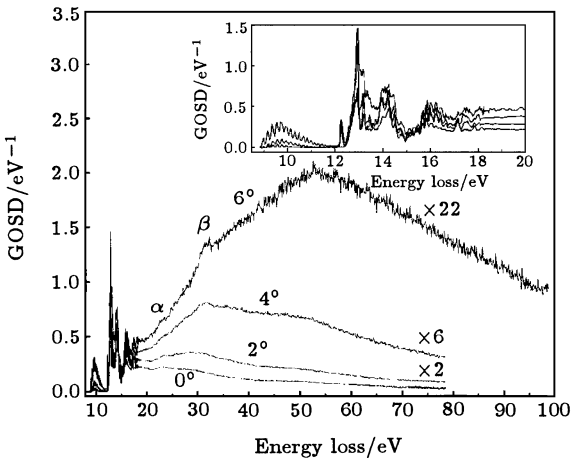


Fig.2. Absolute GOSD spectra of N_2 below 100eV. α and β represent the superexcited states observed in the present experiment. The inset shows the expanded spectra in the energy region of 8.5–20eV.

As for the broad peak around 23eV shown in Fig.3, marked as α in Fig.2, it extends approximately from 22 to 24eV and its intensity sharply decreases with the increasing of the scattering angle. This broad peak was also observed in the fluorescence spectrum,[20] and in the electron energy loss spectra.[21] Therein it was tentatively assigned to the vibrational progression of the doubly excited $(C^2\Sigma_u^+)4s\sigma_g$ and $5s\sigma_g$ Rydberg states converging on the $N_2^+(C^2\Sigma_u^+)$ (R(C)) state. According to Ref.[21], the broad peak in the present spectra mainly comes from the contribution of $(C^2\Sigma_u^+)4s\sigma_g$ Rydberg state, thus the weak $(C^2\Sigma_u^+)5s\sigma_g$ Rydberg state is ignored. The GOSs for this double excitation were obtained and are shown in Fig.4. Clearly, the GOS quickly decreases with the increasing of K^2, which is the typical behaviour of dipole-allowed transition. The behaviour can be understood as follows. Based on Fermi's golden rule, the transition strength is proportional to the square of the transition matrix element, i.e. the transition-operator-weighted overlap integral between the initial ground state and the final doubly excited state. At large angles (e.g., θ=4° and 6°), the transition matrix element results mainly from the interactions in the inner region. At small angles (e.g., θ=0° and 2°), the transition matrix element results mainly from the interactions in the outer region. The wavefunction of the doubly excited Rydberg state with strong repulsive character[20] mostly distributes in the outer region, thus its intensity should decrease faster as K^2 increases. A similar phenomenon has been studied in our previous work for He.[22]

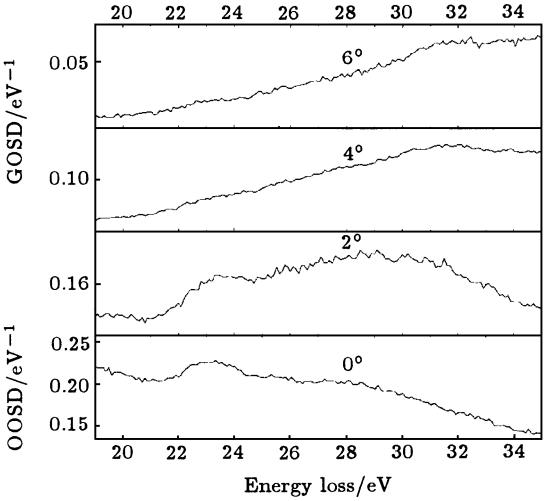


Fig.3. Absolute GOSD spectra of N_2 between 19 and 35eV at the scattering angles of 0°, 2°, 4° and 6°.

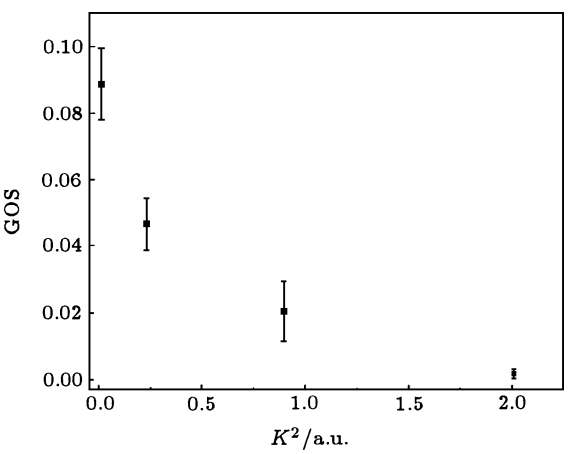


Fig.4. Absolute GOS for the excitation at 23eV in N_2.

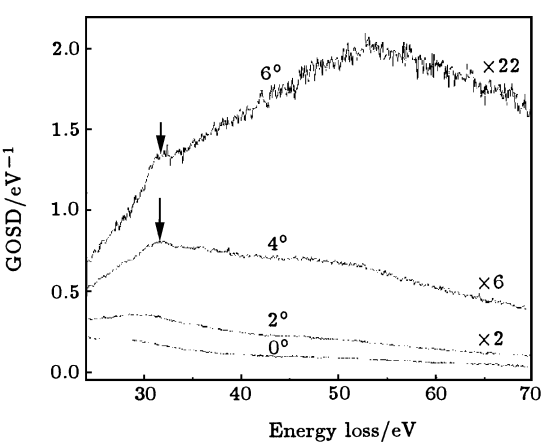


Fig.5. Absolute GOSD spectra of N_2 in the energy region of 20–70eV.

With regard to the broad peak at 31.4eV marked as β in Fig.2, it was not clearly observed until the scattering angle reaches to 4° ($K^2 \sim 0.9$ a.u.) as shown

in Fig.5. This peak was first observed by Lee *et al*[4] and its GOS was determined. More recently, the GOS for this peak was studied by de Souza *et al*[5] both experimentally and theoretically. Based on the above investigations, this peak is assigned to a dipole-forbidden quadrupole–allowed singly excited $^1\Pi_g$ state with the electronic configuration of $(2s\sigma_g)^{-1}(2p\pi_g)^1$. In the present work, the GOSs for this peak were also determined as shown in Fig.6. It can be seen that the three experimental results agree well within the experimental errors. Moreover, we got its GOS at nearly $K^2 \approx 0$. The present results further imply that the peak is a dipole-forbidden quadrupole-allowed transition.

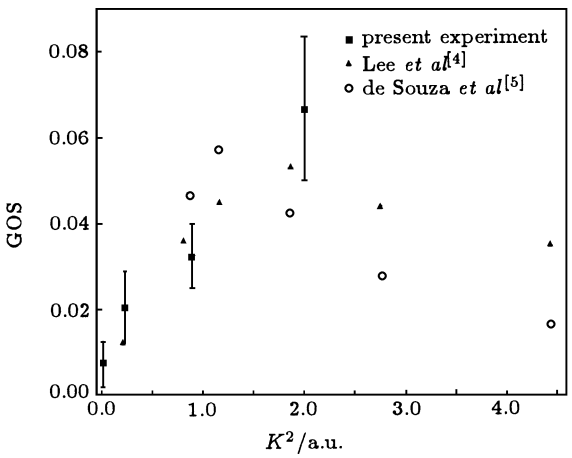


Fig.6. Absolute GOS for the excitation at the 31.4eV in N_2.

4. Conclusion

The absolute OOSD and GOSD spectra of N_2 below 100eV have been determined, and the GOSs for two transitions to the superexcited states at 23 and 31.4eV are reported. More specifically, the GOSs for the transition to the superexcited state at 23 eV are obtained for the first time and the momentum transfer dependence behaviour is discussed.

References

[1] Chan W F, Cooper G, Sodhi R N S and Brion C E 1993 *Chem. Phys.* **170** 81

[2] Xu K Z, Zhong Z P, Wu S L, Feng R F, Ohtani S, Takayanagi T and Kimota A 1995 *Sci. Chin.* (Series A) **38** 368

[3] Brunger M J and Buckman S J 2002 *Phys. Rep.* **357** 215

[4] Lee J S, Wong T C and Bonham R A 1975 *J. Chem. Phys.* **63** 1643

[5] de Souza G G B, Bielschowsky C E, Lucas C A and Souza A C A 1990 *Phys. Rev.* A **42** 1363

[6] Wu S L, Zhong Z P, Feng R F, Xing S L, Yang B X and Xu K Z 1995 *Phys. Rev.* A **51** 4494

[7] Xu K Z, Feng R F, Wu S L, Ji Q, Zhang X J, Zhong Z P and Zheng Y 1996 *Phys. Rev.* A **53** 3081

[8] Zhu L F, Zhong Z P, Ji Q, Zhang X J, Wu S L, Feng R F and Xu K Z 1997 *Acta Phys. Sin.* **46** 458 (in Chinese)

[9] Zhong Z P, Wu S L, Xu Z, Zhu L F, Zhang X J, Feng R F and Xu K Z 1998 *Acta Phys. Sin.* **47** 419 (in Chinese)

[10] Liu X J, Zhu L F, Jiang X M, Yuan Z S, Cai B, Chen X J and Xu K Z 2001 *Rev. Sci. Instrum.* **72** 3357

[11] Zhu L F, Zhong Z P, Yuan Z S, Zhang W H, Liu X J, Jiang X M, Xu K Z and Li J M 2002 *Chin. Phys.* **11** 1149

[12] Chan W F, Cooper G and Brion C E 1991 *Phys. Rev.* A **44** 186

[13] Bethe H 1930 *Ann. Phys.* (Leipzig) **5** 325
Bethe H 1930 *Z. Phys.* **76** 293

[14] Inokuti M 1971 *Rev. Mod. Phys.* **43** 297

[15] Olney T N, Cann N M, Cooper G and Brion C E 1997 *Chem. Phys.* **223** 59

[16] Wheeler J A and Bearden J 1934 *Phys. Rev.* **46** 755

[17] Dehmer J L, Inokuti M and Saxon R P 1975 *Phys. Rev.* A **12** 102

[18] Sun J M, Zhong Z P, Zhu L F, Li W B, Liu X J, Yuan Z S and Xu K Z 2004 *Phys. Rev.* A **70** 012708

[19] Fan L L, Zhong Z P, Zhu L F, Liu X J, Yuan Z S, Sun J M and Xu K Z 2005 *Phys. Rev.* A **71** 032704

[20] Ukai M, Kameta K, Kouchi N, Hatano Y and Tanaka K 1992 *Phys. Rev.* A **46** 7019

[21] Odagiri Takeshi, Takahashi Ken, Yoshikawa Kazuhiro, Kouchi Noriyuki and Hatano Yoshihiko 2001 *J. Phys.* B: *Mol. Opt. Phys.* **34** 4889

[22] Liu X J, Zhu L F, Yuan Z S, Li W B, Cheng H D, Huang Y P, Zhong Z P, Xu K Z and Li J M 2003 *Phys. Rev. Lett.* **91** 193203